

## The Use of Ensembles to Identify Forecasts with Small and Large Uncertainty

ZOLTAN TOTH,\* YUEJIAN ZHU,\* AND TIMOTHY MARCHOK\*

*National Centers for Environmental Prediction, Camp Springs, Maryland*

(Manuscript received 18 May 2000, in final form 2 March 2001)

### ABSTRACT

In the past decade ensemble forecasting has developed into an integral part of numerical weather prediction. Flow-dependent forecast probability distributions can be readily generated from an ensemble, allowing for the identification of forecast cases with high and low uncertainty. The ability of the NCEP ensemble to distinguish between high and low uncertainty forecast cases is studied here quantitatively. Ensemble mode forecasts, along with traditional higher-resolution control forecasts, are verified in terms of predicting the probability of the true state being in 1 of 10 climatologically equally likely 500-hPa height intervals. A stratification of the forecast cases by the degree of overall agreement among the ensemble members reveals great differences in forecast performance between the cases identified by the ensemble as the least and most uncertain. A new ensemble-based forecast product, the “relative measure of predictability,” is introduced to identify forecasts with below and above average uncertainty. This measure is standardized according to geographical location, the phase of the annual cycle, lead time, and also the position of the forecast value in terms of the climatological frequency distribution. The potential benefits of using this and other ensemble-based measures of predictability is demonstrated through synoptic examples.

### 1. Introduction

During the past decade, ensemble forecasting has become an integral part of numerical weather prediction (NWP). Major meteorological centers now regularly produce and use ensemble forecasts (Molteni et al. 1996; Toth and Kalnay 1993; Rennick 1995; Houtekamer et al. 1996; Kobayashi et al. 1996). The role of ensemble forecasting will likely expand in the coming years within the National Weather Service where the use of probabilistic weather, water, and climate forecasts has been adopted as one of the strategic goals to be achieved by 2005 (NWS 1999). One of the main advantages of ensemble forecasting is that it can potentially provide case-dependent estimates of forecast uncertainty (Ehrendorfer 1997). To what extent this promise is fulfilled by the current National Centers for Environmental Prediction (NCEP) global ensemble forecast system (Toth and Kalnay 1997) is the main topic of the present study.

The generation and verification of probabilistic forecasts based on ensembles was the subject of a number

of recent studies (e.g., Anderson 1996; Hamill and Colucci 1997; Talagrand et al. 1997; Eckel and Walters 1998; Atger 1999; Richardson 2000). General statistics for the performance of the NCEP ensemble forecasting system were provided by Zhu et al. [(1996), with a comparison to that of the European Centre for Medium-Range Weather Forecasts’s (ECMWF) Ensemble Prediction System], and Toth et al. [(1998); with a comparison to that of a single higher-resolution control forecast]. These earlier studies demonstrated that the ensemble forecasts can be used to generate skillful probabilistic forecasts, which, after a simple statistical postprocessing based on verification statistics from the recent past, become very reliable.

In recent studies (Mylne 1999; Richardson 2000; Zhu et al. 2001, hereafter ZTW) it was also demonstrated that the potential economic value associated with the use of an ensemble forecasting system may be considerably greater than that attainable by using a single, even-higher-resolution control forecast, given substantial uncertainty in the forecasts (i.e., 500-hPa height forecasts at and beyond 3 days). Note that in the above comparisons neither the ensemble nor the control forecasts were statistically corrected or postprocessed. It was also shown (Toth et al. 1998) that the extra value associated with an ensemble of forecasts as compared to a single control forecast is due to two main factors: 1) the ensemble can characterize foreseeable, flow-dependent variations in the uncertainty of the forecasts, and

---

\* Additional affiliation: General Sciences Corporation, Beltsville, Maryland.

---

*Corresponding author address:* Zoltan Toth, Environmental Modeling Center, NCEP, 5200 Auth Rd., Room 207, Camp Springs, MD 20746.

E-mail: Zoltan.Toth@noaa.gov

2) the ensemble can provide a probability distribution that is more complete than a dichotomous probability description given by a single forecast.

With appropriate postprocessing using past verification statistics, a full probability distribution can be generated from a single control forecast (see, e.g., Talagrand et al. 1997; O. Talagrand 1999, personal communication). Talagrand's results indicated, however, that post-processed full probabilistic forecast distributions based on a single control forecast still did not reach the resolution skill level of that provided by a statistically uncorrected ensemble of forecasts, attesting to the value of case-dependent uncertainty information provided by the ensemble. In a recent study, Atger (2001) attempts to render case-dependent variations in forecast uncertainty to a single forecast, depending on its spatial and temporal structure. If and to what degree such a statistical approach can compete with an ensemble of forecasts based on the estimated initial value uncertainty and its dynamical evolution (Ehrendorfer 1997) is to be evaluated.

In this paper we investigate the extent to which an ensemble of forecasts can distinguish between forecast situations with lower or higher than average expected uncertainty, based on their flow-dependent level of similarity or dissimilarity. Ensemble forecasts over a period of a season (section 2) will be stratified according to the degree of ensemble forecast similarity (section 3). The main results of this study will be presented in section 4. Based on these results, section 5 introduces a new forecast product, the "relative measure of predictability." In section 6, the use of different measures of predictability is demonstrated through synoptic examples, while the conclusions and discussion are given in section 7.

## 2. Ensemble forecast data

In the present study, the NCEP operational global ensemble forecasts (Toth and Kalnay 1997) will be evaluated over the period March–May 1997. The aim here is to assess the extent to which ensemble forecasts can distinguish between cases of higher or lower than average uncertainty. The studied period is from a transition season that coincides with that of Toth et al. (1998). Note that predictability in a transition season is typically lower than in winter but higher than in summer.

The NCEP global ensemble forecasts in 1997 consisted each day of 17 individual forecasts run out to 16 days lead time, of which 3 were control forecasts started from unperturbed analyses, and 14 were perturbed forecasts started from initial conditions where bred perturbations of the size of estimated analysis uncertainty were both added to, and subtracted from the control analyses at 0000 and 1200 UTC (Toth and Kalnay 1997). In section 4, the 14 T62 resolution perturbed forecasts (10 from 0000 UTC, and 4 from 1200 UTC) are evaluated, along with the 0000 UTC Medium-Range Forecast

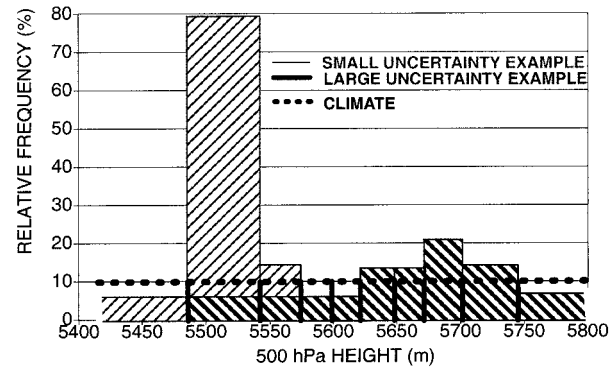


FIG. 1. Ten climatologically equally likely intervals, marked by heavy vertical lines, for a grid point at  $40^{\circ}\text{N}$ ,  $95^{\circ}\text{W}$ , for 500-hPa height for Apr, based on the NCEP–NCAR reanalysis data. In reality the intervals on the two sides are open ended; in the figure they end at the 1% frequency level. Beyond the level of climatological frequency (10% in the vertical scale, dotted horizontal line), two ensemble distributions as examples for low (lightly hatched) and high (heavily hatched) uncertainty cases are also indicated.

(MRF) T126 high-resolution control forecast that provides a reference level of skill.

The 500-hPa height forecast and analysis data will be used over the Northern Hemisphere extratropics ( $20^{\circ}$ – $77.5^{\circ}\text{N}$ ), on a  $2.5^{\circ}$  by  $2.5^{\circ}$  latitude–longitude grid. As in Zhu et al. (1996), and Toth et al. (1998), the forecast and verifying analysis data will be binned at each grid point into 10 climatologically equally probable intervals (Fig. 1). These intervals were defined uniquely for each grid point and each month of the year using the NCEP–National Center for Atmospheric Research (NCAR) reanalysis data (Kalnay et al. 1996). They were then linearly interpolated in time to each date within the study period.

## 3. Methodology

### a. Stratification by expected uncertainty

On each day and at each grid point in the period and region studied, the distribution of the 14 ensemble forecasts at each lead time is evaluated in terms of the 10 climatologically equally likely bins. In particular, the number of ensemble forecast members associated with the most highly populated climate bin is noted. The population in this bin is the *mode* ( $m$ ) of the ensemble distribution, and its value for a 14-member ensemble given in 10 climatologically equally likely bins varies between 2 and 14. The frequency distribution of the mode values over all grid points and all case days is denoted by  $f(m)$ . High ensemble mode values (14, or close to 14) correspond to a compact ensemble, where most members indicate very similar height values, whereas low ensemble mode values (2, or close to 2) indicate a diverse ensemble with little agreement among the members. The former cases generally represent fore-

cast situations with a small ensemble spread, with presumably *small* forecast uncertainty, while the latter cases are characterized by large ensemble spread, presumably indicating *high* forecast uncertainty (see two forecast distribution examples in Fig. 1).

To evaluate the ability of the ensemble to distinguish between forecast cases with low and high uncertainty, 10%–15% ( $P = 0.1$ – $0.15$ ) of the total number of cases (over all grid points and days) associated with the highest and lowest ensemble mode values are identified for all lead times. This is achieved by selecting all grid points separately for which  $m \leq M_l$  (presumed low predictability) and

$$\sum_{m=2}^{M_l} f(m) = P, \quad (1)$$

and for which  $m \geq M_h$  (presumed high predictability) and

$$\sum_{m=M_h}^{14} f(m) = P. \quad (2)$$

At short lead times the ensemble spread is generally small, and thus  $M_h$  is typically large (close or equal to 14). As the lead time increases, the ensemble spread also increases and consequently  $M_h$  decreases. For the subset of cases with the lowest ensemble mode, at long lead time,  $M_l = 2$  or only slightly higher. At shorter lead times with concomitantly smaller ensemble spread,  $M_l$  must be larger to account for approximately the same fraction (10%–15%) of all cases.

### b. Measure of performance

The 10%–15% of cases with the highest and lowest ensemble mode values will be referred to as the “low uncertainty” (or high predictability) and “high uncertainty” (or low predictability) cases, respectively. Charts outlining the geographical areas associated with these cases can be made available in real time to the forecasters (see section 5). The main results of this study shown in the next section pertain to the performance of categorical ensemble mode forecasts, evaluated separately for the high and the low predictability cases as defined above. In addition, the average performance of the control MRF forecasts, which without statistical post-processing cannot be objectively classified into high or low predictability cases, will also be evaluated. The performance measure used for evaluating both the ensemble mode and MRF control forecasts is the average success rate of the particular categorical forecast system:

$$SR = \frac{h_f}{t_f}, \quad (3)$$

where  $h_f$  is the number of cases (hits) when a forecast system, calling for the occurrence of a particular climate bin, correctly verified, and  $t_f$  is the total number of all

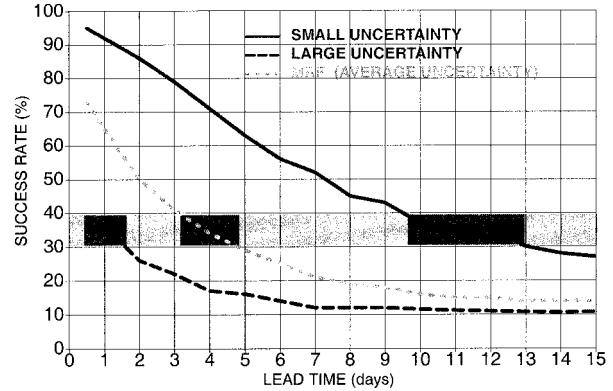


FIG. 2. Average success rate of 500-hPa height ensemble mode forecasts for Mar–May 1997, verified in terms of 10 climatologically equally likely bins at each grid point over the Northern Hemisphere extratropics. The results are stratified into low (continuous line) and high uncertainty (dashed line) groups, according to the number of ensemble members falling into the most populated bin. Each line represents average results for 10%–15% of all cases with the lowest or highest forecast uncertainty, respectively. Success rates for the unstratified high-resolution MRF control forecast are also shown (dotted line). For an explanation of shading, see text.

such forecasts, *accumulated over all climate bins*. In section 4 success rate results for the MRF control forecast (averaged over all cases), and for ensemble mode forecasts evaluated separately over the high and low predictability cases, will be shown. Note that when there are more than one climate bins associated with the value of the ensemble mode, the verification result for one such bin, selected arbitrarily among them, will be included in the statistics.

The success rate as defined above is the complement of the false alarm rate ( $SR = 1 - FAR$ ) and is called *postagreement* in the older literature (see Wilks 1995). In general the performance of a system forecasting a particular event (any 1 particular bin out of 10 climate bins) can be described by a  $2 \times 2$  contingency table (defined by yes/no alternatives for both forecast and observed events), or alternatively, three independent measures based on such a table. Since the event to be predicted in our case has a climatological frequency of 0.1, and the overall forecast frequency of any particular bin (barring any significant model bias) is also 0.1, the success rate [Eq. (1)] uniquely describes the performance of the forecast systems when integrated over all 10 climate bins. If the ensemble mode forecasts exhibit resolution, case-dependent probabilistic categorical forecasts can be issued (section 5).

### c. Attributes of probabilistic forecasts

The two main attributes of probabilistic forecasts are their reliability and resolution (see, e.g., Stanski et al. 1989). Reliability implies that forecast probability values match the conditional observed frequencies of the same events over the long run; for example, forecasts

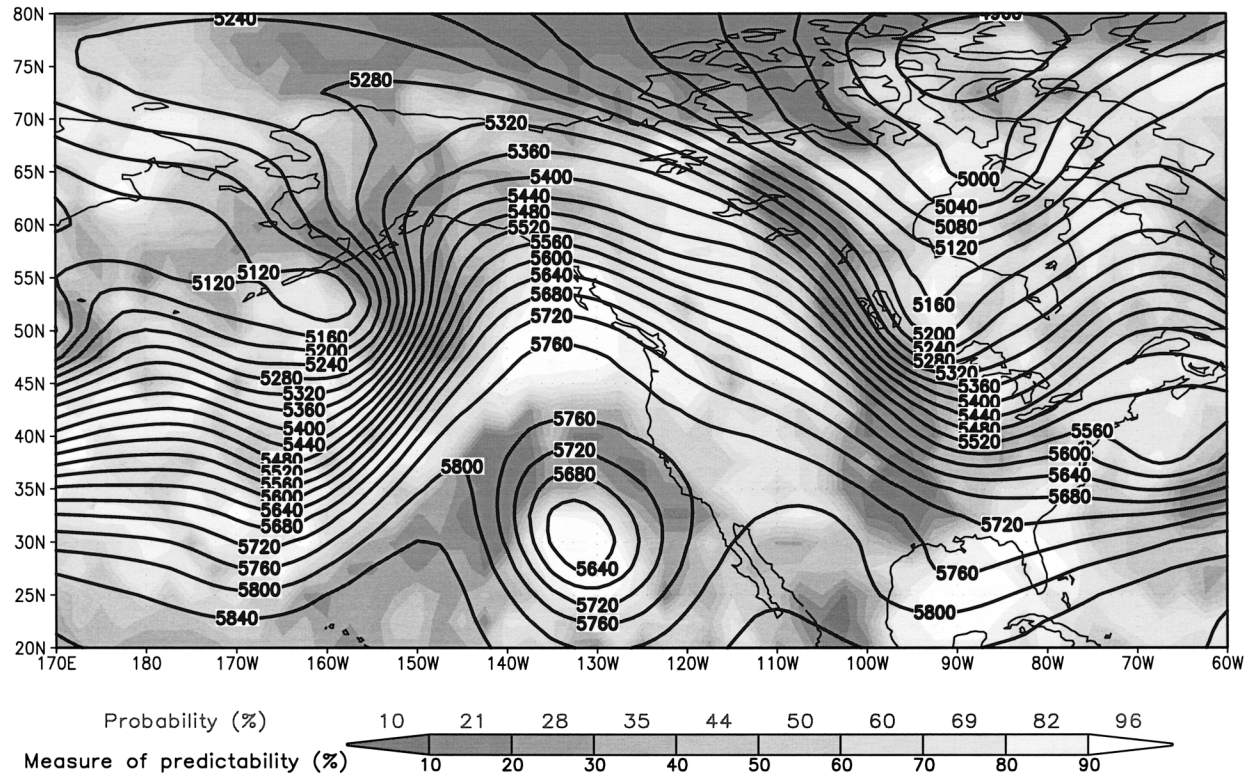


FIG. 3. The 1-day lead time 500-hPa height 10-member NCEP global ensemble mean forecast (contour lines) and associated relative measure of predictability and probabilistic forecast for the climate decile that contains the ensemble mean (gray shades), valid 0000 UTC 5 Dec 2000. For further explanation, see text.

issued with a 40% probability verify 40% of the time. Reliability, however, does not necessarily imply value. For example, if the climate probability of the predicted event is also 40%, the forecast would not have value with respect to using climatological information only. Assuming perfect reliability, resolution is a measure of how “sharp” the probabilistic forecasts are, that is, how close the forecast probability values are to the ideal 0 and 1 values. Perfect resolution (i.e., the exclusive use of 0 and 1 probability values, as with the use of a single control forecast), however, does not guarantee optimal forecasts either, unless accompanied by perfect reliability. An ideal probabilistic forecast system in fact has as much resolution as possible, while exhibiting perfect reliability at the same time.

We know from earlier verification studies (e.g., Zhu et al. 1996; Toth et al. 1998) that probabilistic forecasts based on an ensemble (or a control) forecast can be easily calibrated to make them very reliable. Probability values based on the relative frequency of ensemble members indicating a particular weather event (say, 6 out of 10 members forecasting 1 of the 10 climatologically equally likely bins) may be adjusted to match the past observed frequency of that event, given the same (in this example, 6) ensemble forecast frequency of the weather event. Calibration amounts to a bias removal in the probability space and can be used to reduce the

effect of model bias and insufficient ensemble spread as long as the system behaves consistently in time.

While ensemble-based probabilistic forecasts can be made almost perfectly reliable through calibration, resolution cannot be improved in such a trivial manner. In this study we evaluate how much resolution ensemble mode forecasts have in terms of their ability to distinguish between forecast cases with low and high uncertainty, based on extremely low and high mode values. Since postagreement (success rate) is used in the next section to evaluate the ensemble’s ability to distinguish between low and high uncertainty categorical forecasts, the reliability of probabilistic forecasts is not considered in the analysis presented in the next section. Reliability and calibration will, however, be discussed in sections 5 and 6 where probabilistic (instead of categorical) forecasts will also be considered.

Let us assume that every time the same set of probability values are used for predicting the 10 climate categories used in this study, except arranged in different ways over the 10 categories. Standard measures of resolution [e.g., the resolution part of the ranked probability skill score, RPSS; see, e.g., Wilks (1995)] would indicate a certain amount of resolution, depending on how different the 10 probability values are from the climatological probability value (10%). Such a forecast system would not be able to distinguish between fore-

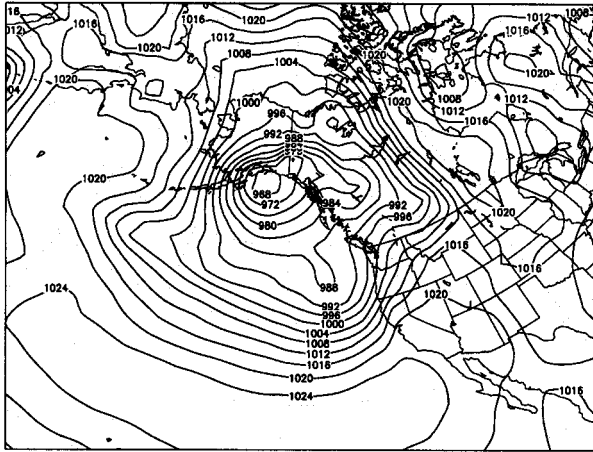


FIG. 4. NCEP analysis of the mean sea level pressure (hPa) field at 1200 UTC 6 Feb 1999.

cast cases with different degrees of predictability. The resolution in such a system can be termed internal to the probability distribution used. The issue of case- (as opposed to the more trivial distribution) dependent resolution can only be addressed with an experimental set-up similar to that used in this study, where the uncertainty associated with a forecast for a single category or event is analyzed. If case-dependent resolution is found, the difference in success rates for the low and high uncertainty cases also provides an easily comprehensible measure of these characteristics of the ensemble. In contrast, values of RPSS scores and other alternative measures are not as straightforward to interpret.

#### 4. Results

As a function of lead time, Fig. 2 evaluates how different the success rates of the forecasts are for the 10%–15% of all cases with the *lowest* and the *highest* predictability, as identified in real time by the ensemble. The average success rate for all cases, using the MRF control forecast, is also shown. Note that the ensemble mode forecasts evaluated for all cases without stratification (not shown) exhibit success rates similar to that of the high-resolution control, except with somewhat lower values before, and somewhat higher values after, day 6 lead time (see Fig. 3 of Toth et al. 1998).

The results indicate that the ensemble forecasting system that was operational in the spring of 1997 had a substantial case-dependent resolution. For example, at 1-day lead time the most predictable 10%–15% of the forecasts verified with a success rate of 92%, while the least predictable 10%–15% verified with a success rate of only 36%. The average success rate for the unstratified MRF forecasts was 65%. The verification statistics at later lead times reveal a somewhat reduced, but still wide, range of success rates. While the overall MRF success rates at 4- (12-) day lead time are 34% (15%),

the most and least predictable 10%–15% of the cases exhibit success rates of 71% and 17% (35% and 11%), respectively. We should keep in mind that a smaller number of less frequently occurring cases with extremely low or high predictability would be associated with verification statistics even more anomalous than those presented in Fig. 2.

Note that the overall average success rates (MRF control, dotted green line in Fig. 2) are closer to the stratified low uncertainty success rates at very short lead time (cf. continuous line at 12 h), and to the high uncertainty success rates at longer lead times (cf. dashed line at longer lead time). The skewness of the success rate distribution is especially prominent at 10-day and longer lead times, suggesting that most of these forecasts are of poor quality, with a smaller number of exceptionally good forecasts.

Beyond exploring the large differences in verification statistics between the most and least uncertain cases at any given lead time, it is also interesting to compare at what lead time forecasts with different levels of uncertainty in Fig. 2 assume the same level of skill. Looking at the range of 0.3–0.4 success rate values highlighted in Fig. 2, we can see for example that the least predictable 10%–15% of the 1-day forecasts have a success rate (36%) that is just about the same as the success rate of 4-day MRF forecasts (34%, average predictability), or the success rate of the most predictable 10%–15% of the 12-day forecasts (35%).

#### 5. Relative measure of predictability

##### a. Motivation

Based on the results above, we consider a new measure of predictability. Ensemble spread has been suggested and evaluated as a possible way to measure flow-dependent errors (see, e.g., Houtekamer 1993; Whitaker and Loughé 1998). This measure, however, has its limitations. Ensemble spread is a function not only of the expected forecast errors but also of the geographical location, phase of the annual cycle, and lead time. Ensemble spread normalized by the spread averaged over a long preceding period over any grid point can reduce the effect of these complicating factors. Another problem is that while small ensemble spread suggests small forecast error (barring errors related to the use of imperfect models), a large local spread value does not necessarily indicate large errors. This is because large spread is a result of intense atmospheric instabilities and the statistically expected level of initial errors. In cases where the initial errors are smaller than expected by the ensemble, however, small local forecast errors can occur (see, e.g., Molteni et al. 1996). Spread should thus be considered as an indication for the upper bound and not for the expected value of the forecast error. This underlines the need for a probabilistic approach when dealing with forecast uncertainty.

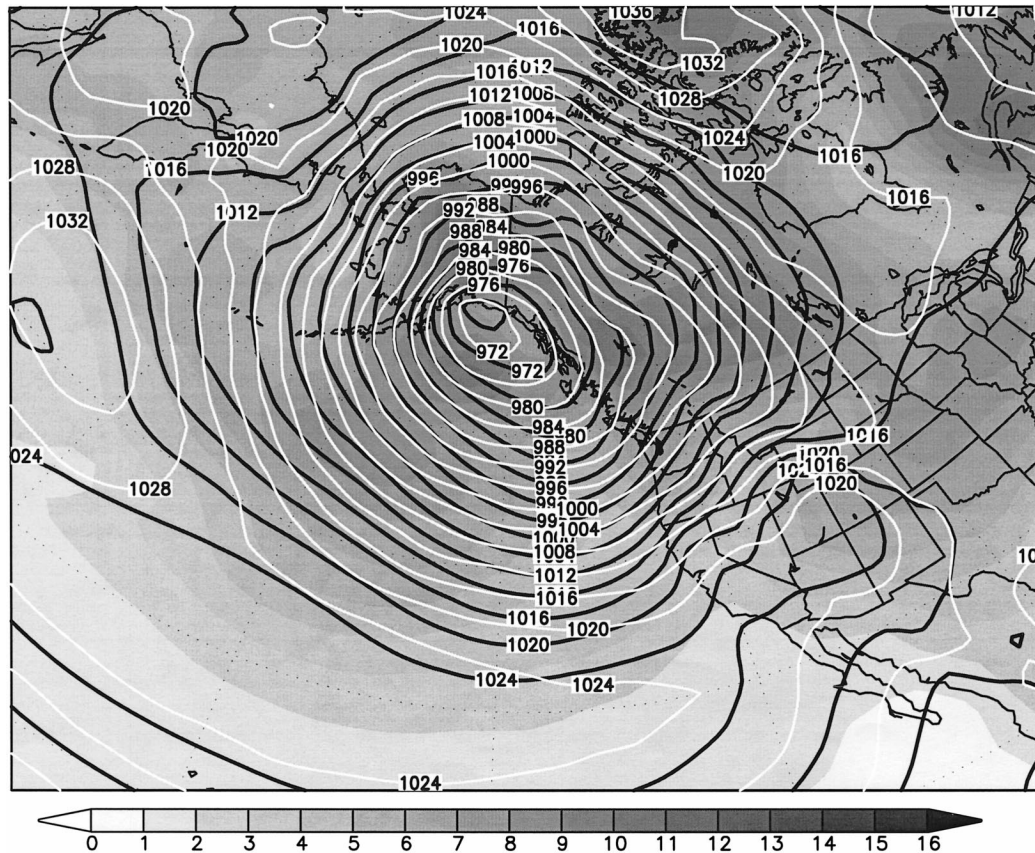


FIG. 5. Operational 9-day NCEP ensemble mean mean sea level pressure (hPa) forecast (white contours) valid at 1200 UTC 6 Feb 1999. The associated spread is indicated by shades of gray. The corresponding operational ECMWF ensemble mean forecast is shown by black contours.

### b. Definition

Here we propose a new, relative measure of predictability to assess the flow-dependent uncertainty in a single forecast. Following the method described in section 3, the new measure is based on the number of ensemble members falling into a particular bin. Since the best (in an rms sense) forecast product is the ensemble mean, unlike in sections 3 and 4, where the bin count for the ensemble mode was evaluated, the bin count for ensemble mean forecasts is considered here.

To construct the new measure, first the mean of the 10 000 UTC members of the NCEP global ensemble forecasts is computed at each grid point (see contour lines in Fig. 3), and the climate bin (Fig. 1) where the mean falls is recorded. The number of ensemble members falling in the bin of the ensemble mean is then counted. Just as in the case of the ensemble mode (Fig. 2), a small (large) number of ensemble members falling into the bin of the ensemble mean (*supporting members*) presumably indicates low (high) predictability. The number of members in that bin is then expressed as a percentile in a frequency distribution of bin counts. This frequency distribution is computed over the preceding

30-day interval,<sup>1</sup> and over the Northern Hemisphere (NH) extratropics. Ten percent (90%) relative predictability at a particular grid point, for example, indicates that 10% (90%) of the grid points had a lower level of predictability during the preceding period over the NH extratropics. These grid points associated with much lower or higher than average predictability were represented by the dashed and continuous success rate curves respectively in Fig. 2 (except that Fig. 2 refers to ensemble mode, and not mean forecasts). These areas of extremely low and high predictability are marked in Fig. 3 by darker and lighter shades of gray, respectively. (A color version of this and other figures can be viewed in a Web version of the present manuscript online at <http://sgi62.wwb.noaa.gov:8080/ens/papers/probpaperw/probpaperw.html>.)

The relative measure of predictability, by construction, is normalized not only by geographical location, season, and lead time but also by the position of the

<sup>1</sup> Instead of weighting every day in the preceding 30-day period equally, we use a recursive filter where the latest day's data are averaged with that for the preceding period with weights of 0.03 and 0.97, respectively. Thus the earlier the data, the less weight it receives.

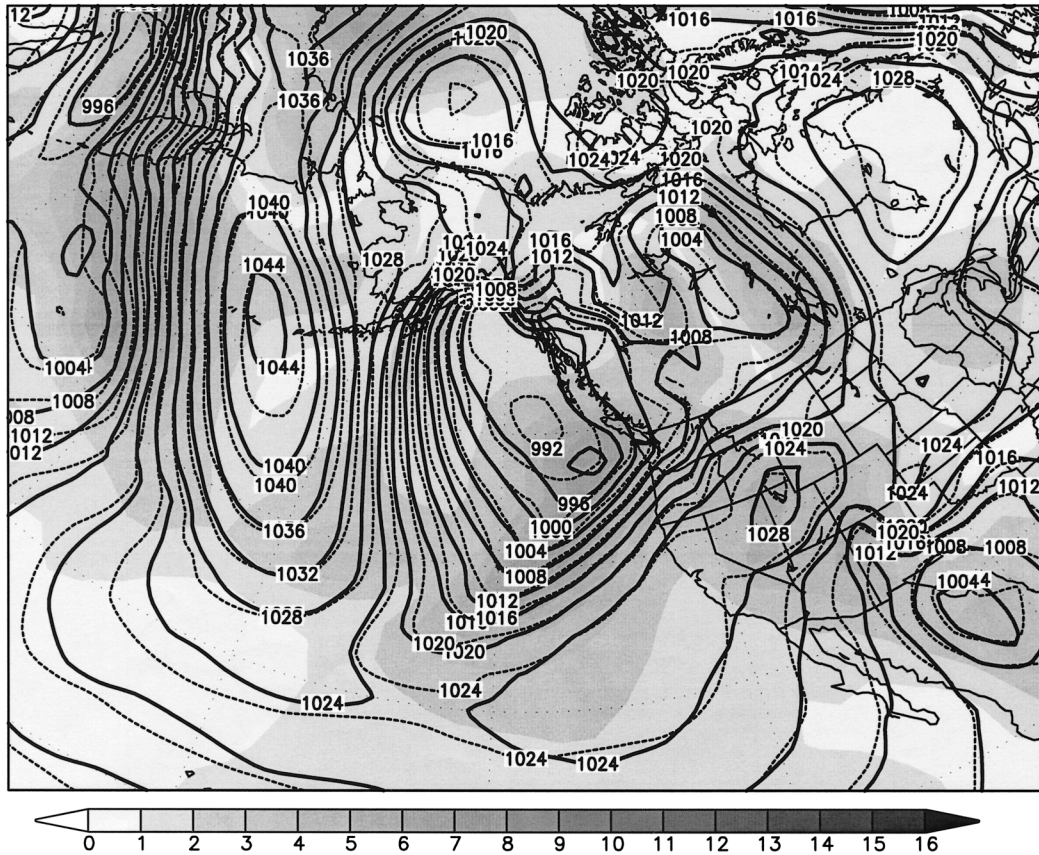


FIG. 6. Same as in Fig. 4 except for 12-h control forecasts valid at 0000 UTC 29 Jan 1999. The NCEP forecast is shown by dashed contours.

forecast value with respect to the climatological distribution. Note that in the case of a climatologically extreme forecast large spread does not necessarily indicate high forecast uncertainty since the variance of observations and forecasts is generally larger for extreme cases (Toth 1992; Ziehmann 2001). By the use of the equiprobable climate intervals that become wider toward the extremes (see Fig. 1), the relative measure of predictability can be interpreted independent of where the forecast is in the climatological distribution.

### c. Probabilistic forecasts

Beyond the various levels of relative predictability, the colors in Fig. 3 are also associated with calibrated probabilistic forecasts for the bin of the ensemble mean. While the relative measure of predictability, by construction, is independent of the lead time and ranges between 0% and 100%, the range of probability values, as suggested by Fig. 2, shrinks and asymptotically tends to the climate probability of 10% when lead time increases. The probability values shown in Fig. 3 are calibrated as described in section 3, using the technique of Zhu et al. (1996) and Toth et al. (1998), based on a preceding 30-day-long independent verification dataset.

Note that the different colors may be associated with more than one bin count. In such cases the calibrated probability value associated with a color is an average of past observed frequency values weighted by the number of points associated with the different bin counts that make up the area with the color in question.

The calibrated probability values reflect forecast uncertainty due not only to initial errors but also to model-related uncertainty. This is another advantage of using probabilistic information (instead of ensemble spread) for assessing forecast uncertainty. Note that while initial value-related uncertainty is determined in a flow-dependent manner based on the ensemble, model-related uncertainty, for the lack of its representation in the NCEP ensemble system, is reflected in the calibrated probabilistic forecasts only in a mean sense, averaged over many cases. In other words, the ensemble-based calibrated probabilistic forecasts reflect uncertainties due to both initial and model errors but resolve *variations* in uncertainty due to initial errors only.

## 6. Synoptic examples

In this section we present three synoptic examples to demonstrate the dramatic variations in the performance

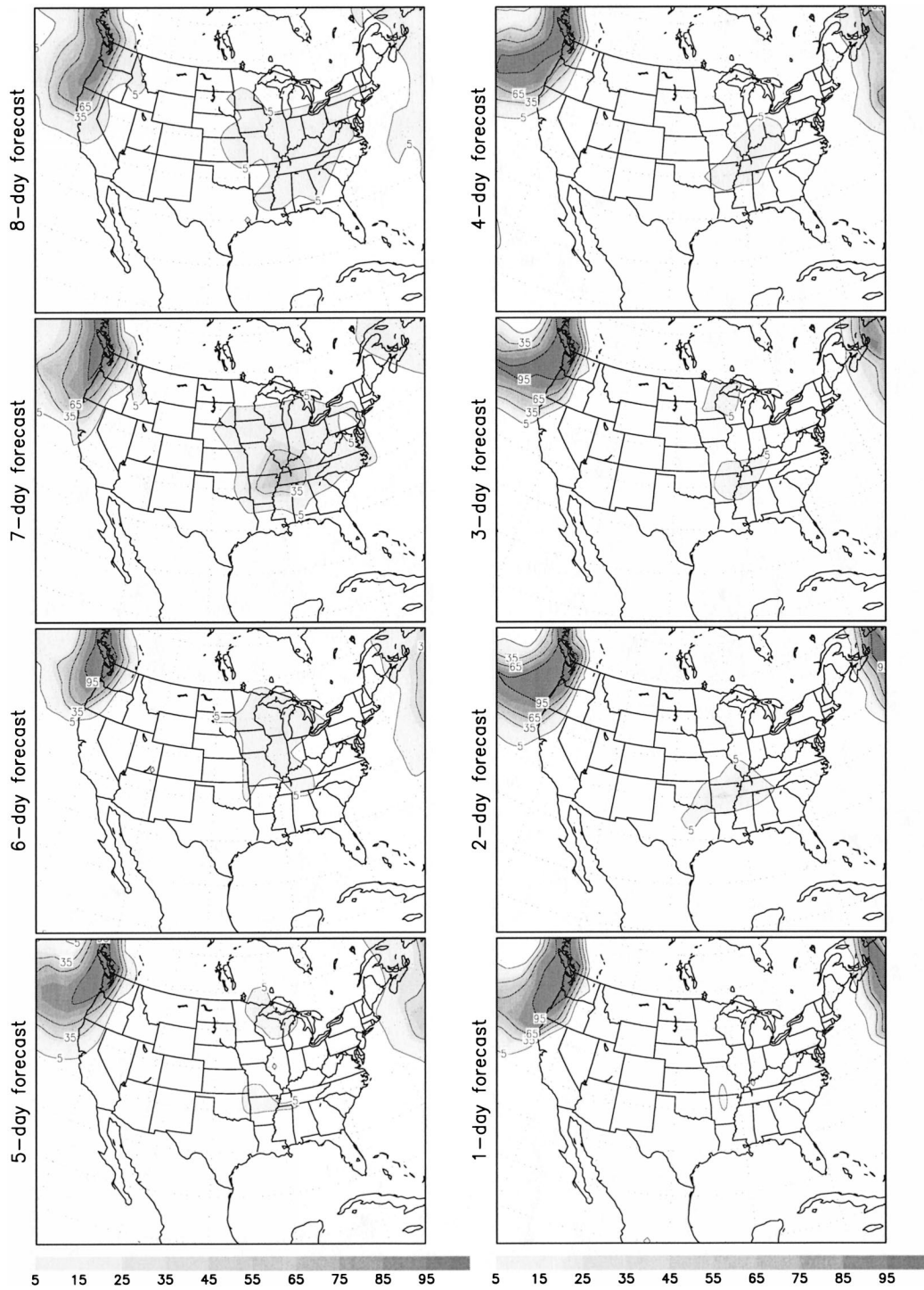


FIG. 7. Probabilistic quantitative accumulated precipitation forecasts for 0.5-in. threshold for a 24-h period ending at 1200 UTC 6 Feb 1999, based on the 17-member NCEP global ensemble forecasts. Forecasts are shown with different lead times (marked as 1-, 2-, . . . , 10-day, initialized at 0000 UTC on 5 Feb and continuing down through 27 Jan). Contour lines are drawn at 5%, 35%, 65%, and 95% probability levels.



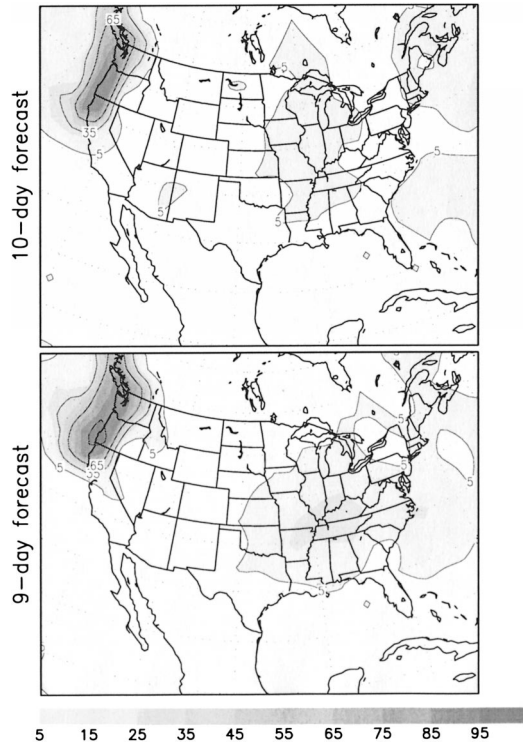


FIG. 7. (Continued)

of NWP forecasts that can be objectively identified using an ensemble forecast system. The specific guidance on above or below average forecast uncertainty (section 5) was introduced only recently. Ensemble spread forecasts that have been accessible since 1997, however, can also be used to identify cases with higher or lower than average predictability. All the examples that follow were identified in real time by the authors. The first two examples—one for extremely high, and another for low predictability—will be presented here in terms of mean sea level pressure ensemble spread and probabilistic quantitative precipitation forecasts, while the third will feature the relative measure of predictability for 500-hPa height forecasts.

#### a. Low uncertainty at long lead time

First we consider a deep low pressure system that developed in the Gulf of Alaska, affecting the U.S. and Canadian west coast around 1200 UTC 6 February 1999. The analyzed mean sea level central pressure of the system had a closed contour of 968 hPa (Fig. 4), indicating a strongly anomalous flow with a 40-hPa negative anomaly from the long-term mean. This cyclone was apparently associated with a very high degree of predictability. It was at 11.5-day lead time when the feature of the anomalous low was first noted in real time using the NCEP ensemble forecasts. And the ensemble mean of the mean sea level pressure forecast did not change much after the initial time of 0000 UTC 27

January (10.5-day lead time), with the deepest closed isobar of the low predicted between 972 and 964 hPa at 9.5-day and shorter lead times.

As an example, in Fig. 5 we present the 9-day NCEP ensemble mean forecast (white contours), along with its associated spread (shades of gray). Over large areas of the storm and its environment, including the extreme central low pressure area, the associated ensemble spread (standard deviation of ensemble members around the mean) remained around or below 6 hPa. This is half or less than half of the average ensemble spread computed for the preceding month at this lead time (not shown), indicating well below average forecast uncertainty. The low level of forecast uncertainty is corroborated by the fact that consecutive ensemble mean and spread forecasts valid at the same time (not shown) were very similar. A comparison of the 9-day ensemble mean forecast (Fig. 5) with the verifying analysis (Fig. 4) reveals that the forecasts for this cyclone, as expected from the real-time uncertainty estimates, verified very well; the error in the central pressure forecasts was only a few hPa.

Comparing the large-scale flow configurations at 12-h (Fig. 6) and 9-day (Fig. 5) lead time it is clear that the forecasts were not trivially persisting the observed features present around initial time. Great changes from extremely high to extremely low anomalous pressure conditions were predicted well over large areas, with changes from initial to final state reaching up to 40 hPa over Alaska and nearby areas. Note that the extremely low height values analyzed in Fig. 4 were well predicted by the ensemble mean forecasts (Fig. 5), documenting that the ensemble mean can retain highly anomalous flow patterns as long as these features are highly predictable.

It is interesting to note that analyzed 500-hPa height values near the center of the storm were around 4777 m with a negative anomaly of more than 500 m, falling into the lowest 1% of historical cases based on the NCEP–NCAR reanalysis. At 9-day lead time, 80% (40%) of all ensemble members fell into the lowest 2% (1%) of the climatological distribution, giving a strong indication for the possible occurrence of extreme low values.

The lower than average ensemble spread in Fig. 5 indicates that all members were rather similar. Therefore it is not surprising that the MRF control forecast also verified well. A user with access to only a single control forecast, however, could not have made much use of a control forecast on its own. Given the low levels of average skill at the 9–11-day lead time (less than 20% success rate, see dotted green curve in Fig. 2), forecasts would be issued with a very low level of confidence, which would render them useless for a wide range of users (see, e.g., Fig. 4 of ZTW). Yet with access to information on the widely varying levels of uncertainty, indicated reliably by the ensemble, there are times when extended-range weather forecasts with much increased

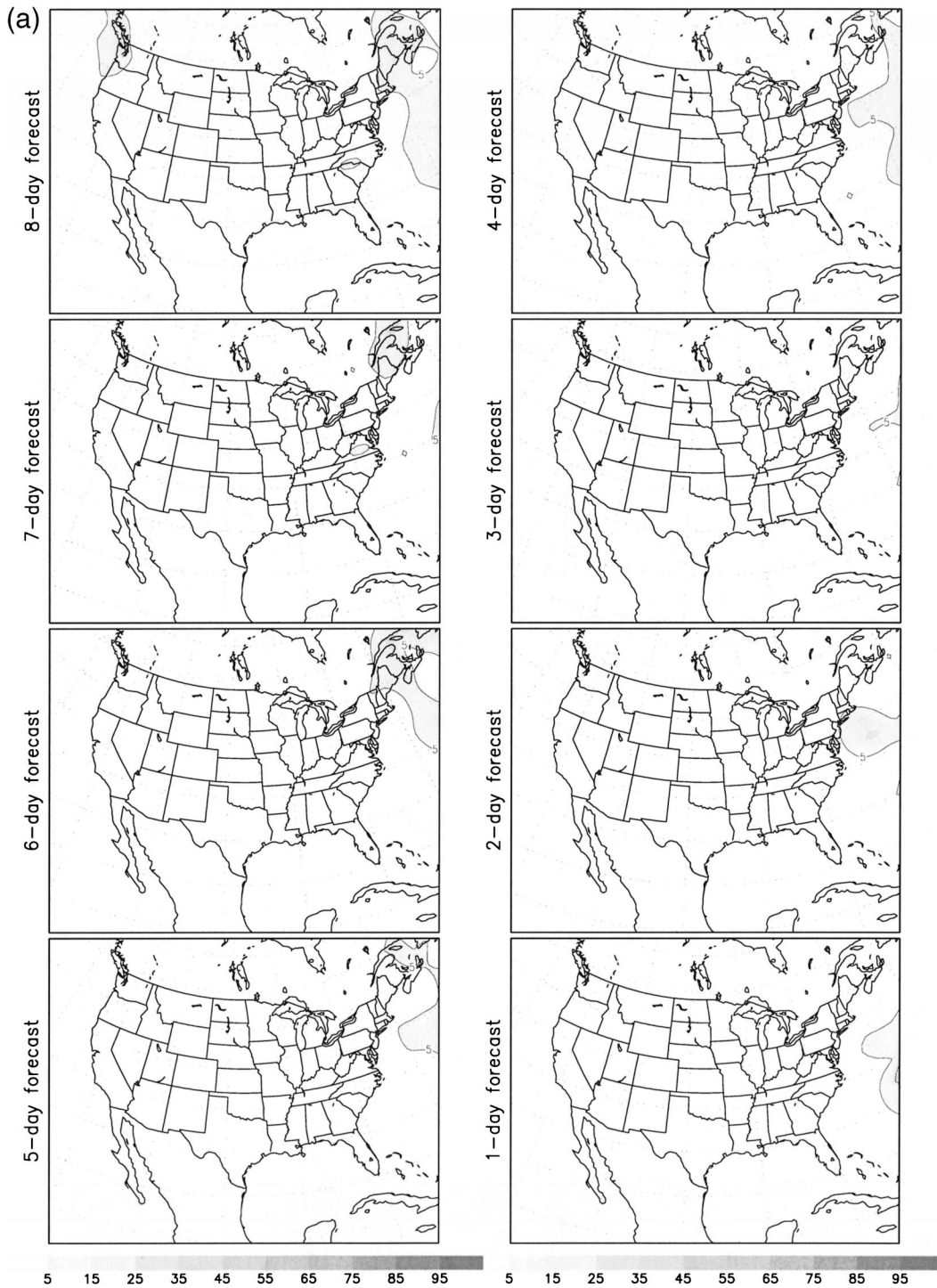


FIG. 8. Same as in Fig. 7 except for 1-in. threshold for periods ending (a) 1200 UTC 5 Feb and (b) 6 Feb 1999, for 1–8-day lead times.

confidence can be made (cf. lightly hatched distribution in Fig. 1, and continuous curve in Fig. 2).

The above case provides such an example, where confident extended range daily sensible weather forecasts could have been issued based on the ensemble guidance.

For example, 12 or more of the 17-member NCEP ensemble forecasts (70%–100%) indicated 0.5 in. or more 24-h accumulated precipitation at 10-day and shorter lead times (Fig. 7) over all areas on the northwest U.S. coast that actually received that much precipitation.

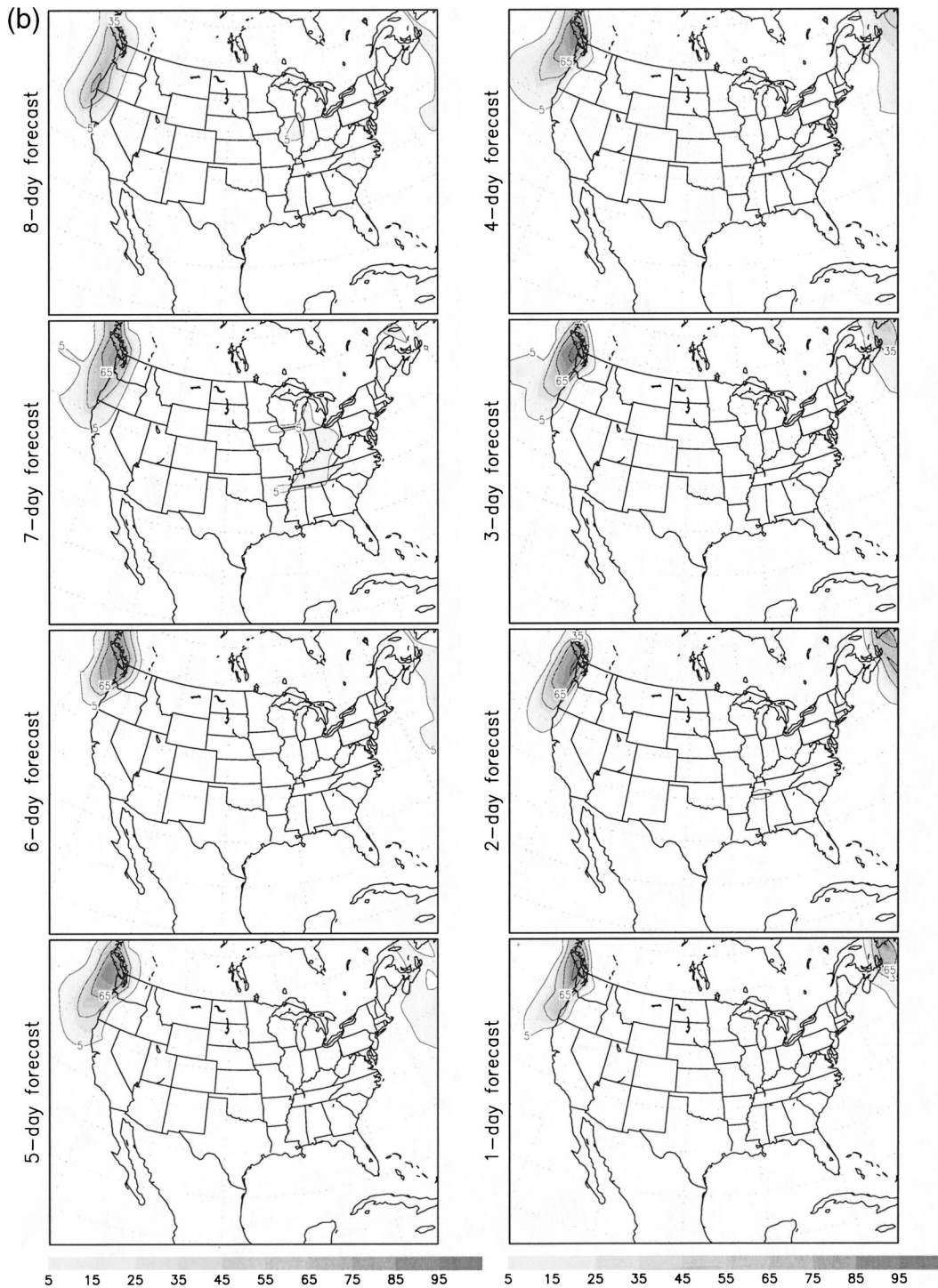


FIG. 8. (Continued)

Similarly, at 7-day or shorter lead times, the ensemble predicted 70% or higher probabilities for most areas affected by more than 1 in. of precipitation (Fig. 8b). The high degree of predictability in terms of accumulated precipitation may be related to the fact that in this case the precipitation is partly orographically forced.

The time evolution of the weather associated with the storm, as suggested by the unusually low ensemble spread over large areas surrounding the storm, was also well predicted. For example, in contrast to the 70% and higher forecast probability of 1 in. or more precipitation corresponding to the observed precipitation event

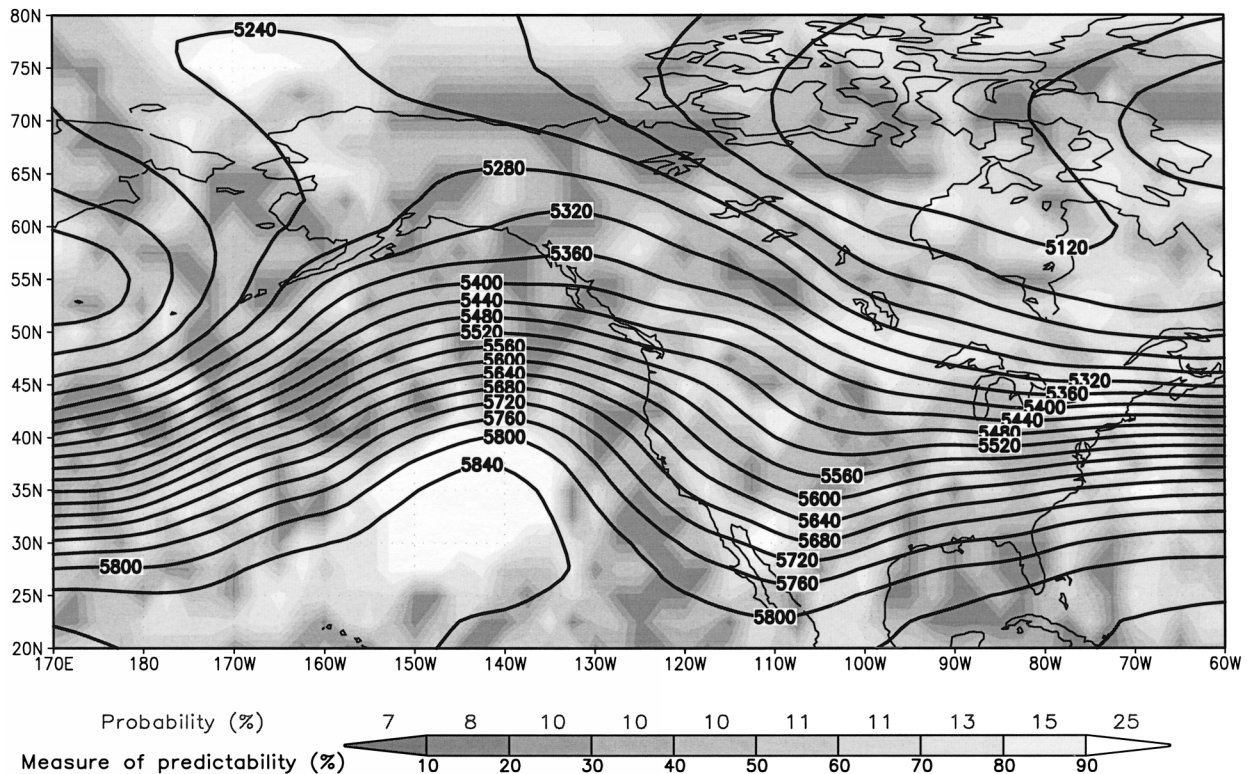


FIG. 9. Same as in Fig. 3 except for an 11-day forecast valid at 0000 UTC 13 Dec 2000.

around 0000 UTC 6 February, the ensemble correctly gave *zero probability* at 7-day and shorter lead times for more than 1 in. of precipitation for the preceding 24-h period, centered around 0000 UTC 5 February (Fig. 8a).

It is important to note that because the NCEP ensemble does not account for model-related uncertainties, small ensemble spread may sometimes be associated with large forecast errors due to model deficiencies. The strong similarity between the NCEP (white contours) and ECMWF (black contours) ensemble mean forecasts, generated by two different models, made the occurrence of such errors in this case less likely (Fig. 5).

#### b. High uncertainty at short lead time

The previous example illustrated the potential value of the ensemble approach in identifying weather features associated with low forecast uncertainty, even at long lead times. In this section, an example is shown of a case with unusually high forecast uncertainty. Identifying these cases can be especially valuable at shorter lead times where the overall level of forecast skill is relatively high. Interestingly, a prominent example of this kind offers itself in the same forecast studied in Fig. 5, but valid at a very short lead time.

Shown in Fig. 6 is the 12-h lead time NCEP high-resolution control forecast (called AVN, solid contours), valid at 0000 UTC 29 January 1999. A closed low,

associated with a cold front extending to the southwest, is seen over the eastern Pacific approaching the west coast of the United States. The ensemble spread associated with this system is around 6 hPa. This is the same level of uncertainty found over large areas of the storm studied in the 9-day forecast example of Fig. 5. But while the 6-hPa spread is half or less of the usual spread at 9-day lead time (Fig. 5), it is up to 3 times more than the usual spread at the 12-h lead time (Fig. 6).

A comparison of the 12-h NCEP control forecast to that from ECMWF (cf. solid and dashed contours in Fig. 6) confirms the unusually high degree of uncertainty regarding the position of the closed low. The largest differences between the two fields, which reach up to 5 hPa, occur in the area of large ensemble spread. The 5-hPa difference observed between the two control forecasts over the eastern Pacific low pressure system at 12-h lead time (Fig. 6) is actually above the level of difference present between the two ensemble mean forecasts 8.5 days later, near the center of the Gulf of Alaska storm where the differences are 4 hPa or less (Fig. 5).

Given the high level of *average* success rate of 12-h forecasts (65%, see dotted green curve in Fig. 2), a weather forecast based on a single control integration in this case may provide misleading guidance in terms of overconfidence. Information again from the ensemble, in this case based on larger than normal spread, may provide case-dependent uncertainty estimates (see

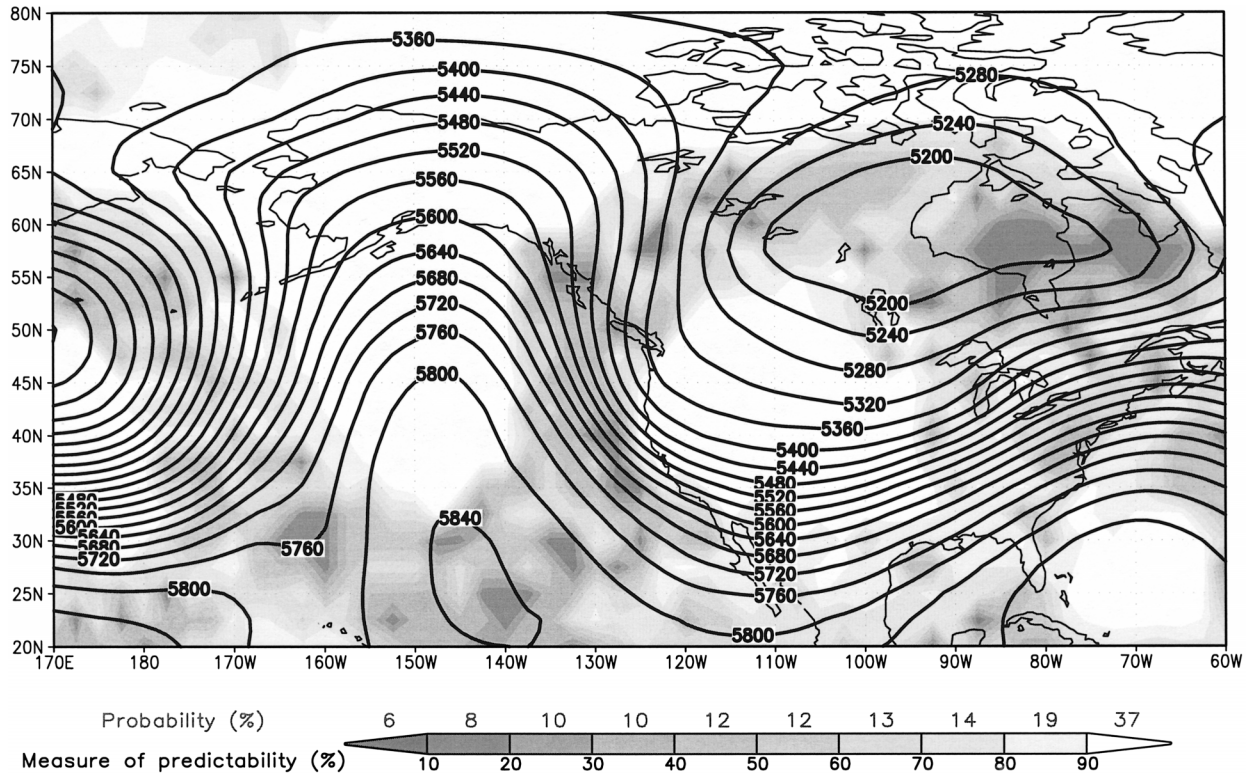


FIG. 10. Same as in Fig. 9 except for a 9-day forecast.

the heavily hatched distribution in Fig. 1, and the dashed curve in Fig. 2), which are helpful for many applications.

The large differences present within the 12-h lead time NCEP ensemble, and between the ECMWF and NCEP control forecasts off the northwest U.S. coast in Fig. 6 (around 6 hPa), would certainly be associated with different weather conditions, with the ECMWF forecast, for example, suggesting stronger onshore winds, associated with heavier precipitation. Note that the same northeast Pacific area in the 9-day forecast (Fig. 5) is associated with the same or lesser degree of uncertainty (5–6-hPa ensemble spread and forecast differences).

It is interesting to note that based on the results of Fig. 2, 10%–15% of the time a 9-day forecast is expected to be more accurate than 12-h forecasts on the least predictable 10%–15% of cases. It follows that the chances that both a high uncertainty 12-h forecast and a low uncertainty 9-day forecast would appear on the same day and in the same area is on the order of 1%–2%. In other words, in an average year and at any location, 4–6 days are expected when a 9-day forecast can be made with the same or slightly higher certainty than a 12-h forecast. As a reference, both of these forecasts would exhibit a skill of the level of an average 3-day forecast.

### c. Emerging forecast features

The example in Fig. 9 displays an 11-day ensemble mean 500-hPa forecast along with the relative measure of predictability and associated probability forecast, valid for 0000 UTC 13 December 2000. The ensemble mean forecast does not have strong anomalies from the climatological mean. Over most of the domain the relative measure of predictability is in the medium to low range, with corresponding probability values close to the 10% climate probability. This suggests, in general, little forecast information in the ensemble, corresponding to a low level of predictability. Figure 10 shows a 9-day forecast with the same valid time. In contrast to Fig. 9, the ensemble mean forecast is highly anomalous and over large areas the relative measure of predictability is in the 90% range. A number of significant features, among them the deep low pressure system around 170°E, the northeast Pacific ridge and the western U.S. trough, are associated with probabilistic forecasts as high as 37%. This indicates, given the long lead time, a relatively high amount of forecast information content with respect to the 10% climatological probability level, which appears just 2 days after the featureless forecast displayed in Fig. 9.

Interestingly, the 24-h forecast (Fig. 3) from the same ensemble as shown in Fig. 9 (initiated at 0000 UTC 4 Dec 2000) indicates a low level of predictability over large

areas where the 9-day forecast is highly predictable. In particular, areas in the Gulf of Alaska and over the mid-United States show forecast probability levels at the 1-day lead time ( $\leq 35\%$ ) below that marked at the 9-day lead time (37%). Similarly to the examples in Figs. 5 and 6, these are areas where an extended-range forecast contains more information than a short-range forecast does. (Real-time forecast maps like those displayed in Figs. 3–10 can be found online at the Environmental Modeling Center's global ensemble Web page: <http://sgi62.wwb.noaa.gov:8080/ens/enshome.html>.)

## 7. Conclusions and discussion

The analysis of the NCEP global ensemble forecast system in sections 3 and 4 was based on verification results of the ensemble mode and higher-resolution control forecasts. Ensemble mode forecasts were stratified according to the value of the ensemble mode, which represents a measure of how tightly or loosely distributed the ensemble members are. The ensemble forecasts were found to possess a substantial amount of case-dependent resolution. Therefore they can reliably indicate, at the time weather forecasts are prepared, the large case to case variations in forecast uncertainty. For example, 10%–15% of the 1-day forecasts identified as the least and most uncertain by the NCEP ensemble have associated success rates of 92% and 36%; the same numbers for 4- (and 12-) day forecasts are 71% and 17% (35% and 11%), respectively.

A further analysis of the results, along with those of other studies (see, e.g., Toth and Kalnay 1995), suggests that on one hand daily weather prediction for the 6–15-day range is possible in cases identified by the ensemble as highly predictable, with the same accuracy and confidence as that of short-range forecasts with poorer than average predictability. As Fig. 5 exemplifies, from time to time even extremely anomalous weather patterns can be forecast with high confidence in the extended range. On the other hand, in flow configurations with unusually low predictability, the skill of short-range forecasts is expected to be as low as average medium-range forecasts, or above average predictability extended-range forecasts. We note that the extreme climate categories, as expected from the statistical considerations of van den Dool and Toth (1991), generally exhibit higher forecast success rates than categories near normal. This aspect of the forecast systems has not been evaluated in the present study where success rates were compounded over all climate bins.

The large variations in forecast uncertainty revealed above are a function of 1) the size and distribution of errors in the analysis fields used to initialize NWP forecasts, and 2) the particular evolution of flow patterns from initial to final forecast times. Variations in forecast uncertainty are a direct consequence of the chaotic nature of the atmosphere and are out of the control of the forecasters. Before the advent of ensemble forecasting,

forecasters had no or very limited advance knowledge of these changes in forecast uncertainty. With ensemble forecasting, as recent studies have demonstrated, these dramatic changes have become routinely predictable.

Based on the above results, NCEP recently introduced, on an experimental basis, geographical displays of probabilistic forecasts for the climate bin in which the ensemble mean falls, out of 10 climatologically equally likely intervals. Areas with above and below average probability values at all lead times are highlighted by lighter and darker shades of gray, respectively (corresponding to the success rates for cases with high and low predictability, like those in Fig. 2). The new measure provides for easy identification of areas with significant deviations from average forecast uncertainty and offers a bridge between traditional single-value (point) forecasts and new, probabilistic type of forecasts.

In the present study ensemble mode forecasts associated with case-dependent estimates of uncertainty were evaluated. Ensemble forecasts, however, can also provide more detailed probability distributions, thus further increasing the potential economic value attainable from the use of weather forecasts. Note that such probabilistic forecasts can also be generated based on single control forecasts (Talagrand et al. 1997; Atger 2001). The value of these forecasts, at least theoretically, is limited compared to that attainable through an ensemble of forecasts that can properly account for forecast uncertainty due to initial value and model related errors. In any case the generation and use of probability distributions, instead of single-value (or categorical) forecasts, requires a conceptual change on the part of the forecaster but this change is necessary for realizing all the benefits an ensemble has to offer.

The performance of NWP forecasts, whether control or ensemble, is negatively affected by the use of imperfect forecast models. The success rates reported in this study, for example, are lower than they would be under ideal conditions, due to simplifications in model formulation. The utility of ensemble forecasts is also limited by shortcomings in the formation of the ensemble. The NCEP ensemble, for example, accounts for forecast uncertainty related only to errors in initial conditions, but not to errors caused by model imperfectness. Therefore the range of foreseeable variations in forecast skill would be wider could we predict the occurrence of flow-dependent random or systematic model errors. The results in this and other studies evaluating operational ensemble forecasts naturally reflect all these limiting factors and represent the currently operationally attainable levels of skill. Under these limiting conditions, the ensembles exhibit great value beyond that of single control forecasts, and are ready to be used by forecasters and end users alike. The fact that the system is not perfect and can be improved in the future should not discourage anyone from taking full advantage of what ensemble forecasting can currently offer.

*Acknowledgments.* We are grateful to David Burridge, director, and the staff of ECMWF, in particular Horst Boettger and John Henessy, for participating in an exchange of ensemble forecasts between ECMWF and NCEP on a research basis. Richard Wobus of GSC provided help with data processing. Steven Tracton, Ed O'Lenic, and Peter Manousos of NCEP; John Jacobson (formerly of GSC); and two anonymous reviewers provided helpful comments on earlier versions of the manuscript.

## REFERENCES

- Anderson, J. L., 1996: A method for producing and evaluating probabilistic forecasts from ensemble model integrations. *J. Climate*, **9**, 1518–1530.
- Atger, F., 1999: The skill of ensemble prediction systems. *Mon. Wea. Rev.*, **127**, 1941–1953.
- , 2001: Verification of intense precipitation forecasts from single models and ensemble prediction systems. *Nonlinear Processes Geophys.*, in press.
- Eckel, F. A., and M. K. Walters, 1998: Calibrated probabilistic quantitative precipitation forecasts based on the MRF ensemble. *Wea. Forecasting*, **13**, 1132–1147.
- Ehrendorfer, M., 1997: Predicting the uncertainty of numerical weather forecasts: A review. *Meteor. Z.*, **6**, 147–183.
- Hamill, T. M., and S. J. Colucci, 1997: Verification of Eta–RSM short-range ensemble forecasts. *Mon. Wea. Rev.*, **125**, 711–724.
- Houtekamer, P. L., 1993: Global and local skill forecasts. *Mon. Wea. Rev.*, **121**, 1834–1846.
- , L. Lefaiivre, J. Derome, H. Ritchie, and H. L. Mitchell, 1996: A system simulation approach to ensemble prediction. *Mon. Wea. Rev.*, **124**, 1225–1242.
- Kalnay, E., and Coauthors, 1996: The NCEP/NCAR 40-Year Reanalysis Project. *Bull. Amer. Meteor. Soc.*, **77**, 437–471.
- Kobayashi, C., K. Yoshimatsu, S. Maeda, and K. Takano, 1996: Dynamical one-month forecasting at JMA. Preprints, *11th Conf. on Numerical Weather Prediction*, Norfolk, VA, Amer. Meteor. Soc., 13–14.
- Molteni, F., R. Buizza, T. N. Palmer, and T. Petroliaigis, 1996: The ECMWF ensemble system: Methodology and validation. *Quart. J. Roy. Meteor. Soc.*, **122**, 73–119.
- Mylne, K. R., 1999: The use of forecast value calculations for optimal decision making using probability forecasts. Preprints, *17th Conf. on Weather Analysis and Forecasting*, Denver, CO, Amer. Meteor. Soc., 235–239.
- NWS, 1999: Vision 2005: National Weather Service Strategic Plan for Weather, Water, and Climate Services 2000–2005. 24 pp. [Available from NWS, 1315 East–West Highway, Silver Spring, MD, 20910-3282.]
- Rennick, M. A., 1995: The ensemble forecast system (EFS). Models Department Tech. Note 2-95, 19 pp. [Available from Models Department, Fleet Numerical Meteorology and Oceanography Center, 7 Grace Hopper Ave., Monterey, CA 93943.]
- Richardson, D. S., 2000: Skill and economic value of the ECMWF ensemble prediction system. *Quart. J. Roy. Meteor. Soc.*, **126**, 649–668.
- Stanski, H. R., L. J. Wilson, and W. R. Burrows, 1989: Survey of common verification methods in meteorology. WMO World Weather Watch Tech. Rep. 8, WMO/TD. No. 358, 114 pp.
- Talagrand, O., R. Vautard, and B. Strauss, 1997: Evaluation of probabilistic prediction systems. *Proc. Workshop on Predictability*, Reading, United Kingdom, ECMWF, 1–25.
- Toth, Z., 1992: Quasi-stationary and transient periods in the Northern Hemisphere circulation series. *J. Climate*, **5**, 1235–1247.
- , and E. Kalnay, 1993: Ensemble forecasting at NMC: The generation of perturbations. *Bull. Amer. Meteor. Soc.*, **74**, 2317–2330.
- , and —, 1995: Ensemble forecasting at NCEP. *Proc. Seminar on Predictability*, Reading, United Kingdom, ECMWF, 39–60.
- , and —, 1997: Ensemble forecasting at NCEP and the breeding method. *Mon. Wea. Rev.*, **125**, 3297–3319.
- , Y. Zhu, T. Marchok, S. Tracton, and E. Kalnay, 1998: Verification of the NCEP global ensemble forecasts. Preprints, *12th Conf. on Numerical Weather Prediction*, Phoenix, AZ, Amer. Meteor. Soc., 286–289.
- van den Dool, H. M., and Z. Toth, 1991: Why do forecasts for “near normal” often fail? *Wea. Forecasting*, **6**, 76–85.
- Whitaker, J. S., and A. F. Lough, 1998: The relationship between ensemble spread and ensemble mean skill. *Mon. Wea. Rev.*, **126**, 3292–3302.
- Wilks, D. S., 1995: *Statistical Methods in the Atmospheric Sciences*. Academic Press, 467 pp.
- Zhu, Y., G. Iyengar, Z. Toth, M. S. Tracton, and T. Marchok, 1996: Objective evaluation of the NCEP global ensemble forecasting system. Preprints, *15th Conf. on Weather Analysis and Forecasting*, Norfolk, VA, Amer. Meteor. Soc., J79–J82.
- , Z. Toth, and R. Wobus, 2001: On the economic value of ensemble based weather forecasts. *Bull. Amer. Meteor. Soc.*, in press.
- Ziehmann, C., 2001: Skill prediction of local weather forecasts based on the ECMWF ensemble. *Nonlinear Processes Geophys.*, in press.